ACS APPLIED MATERIALS & INTERFACES

Research Article

www.acsami.org

Contrasting Performance of Donor–Acceptor Copolymer Pairs in Ternary Blend Solar Cells and Two-Acceptor Copolymers in Binary Blend Solar Cells

Petr P. Khlyabich, Andrey E. Rudenko, Beate Burkhart, and Barry C. Thompson*

Department of Chemistry and Loker Hydrocarbon Research Institute, University of Southern California, Los Angeles, California 90089-1661, United States

Supporting Information

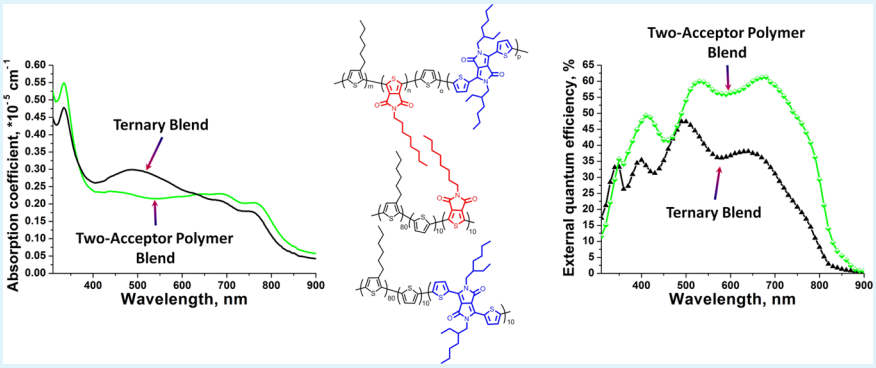

ABSTRACT: Here two contrasting approaches to polymer–fullerene solar cells are compared. In the first approach, two distinct semi-random donor–acceptor copolymers are blended with phenyl-C_{61}-butyric acid methyl ester ($PC_{61}BM$) to form ternary blend solar cells. The two poly(3-hexylthiophene)-based polymers contain either the acceptor thienopyrroledione (TPD) or diketopyrrolopyrrole (DPP). In the second approach, semi-random donor–acceptor copolymers containing both TPD and DPP acceptors in the same polymer backbone, termed two-acceptor polymers, are blended with $PC_{61}BM$ to give binary blend solar cells. The two approaches result in bulk heterojunction solar cells that have the same molecular active-layer components but differ in the manner in which these molecular components are mixed, either by physical mixing (ternary blend) or chemical "mixing" in the two-acceptor (binary blend) case. Optical properties and photon-to-electron conversion efficiencies of the binary and ternary blends were found to have similar features and were described as a linear combination of the individual components. At the same time, significant differences were observed in the open-circuit voltage (V_{oc}) behaviors of binary and ternary blend solar cells. While in case of two-acceptor polymers, the V_{oc} was found to be in the range of 0.495–0.552 V, ternary blend solar cells showed behavior inherent to organic alloy formation, displaying an intermediate, composition-dependent and tunable V_{oc} in the range from 0.582 to 0.684 V, significantly exceeding the values achieved in the two-acceptor containing binary blend solar cells. Despite the differences between the physical and chemical mixing approaches, both pathways provided solar cells with similar power conversion efficiencies, highlighting the advantages of both pathways toward highly efficient organic solar cells.

KEYWORDS: *solar cell, ternary blend, semi-random copolymer, two-acceptor polymer, organic alloy, open-circuit voltage*

INTRODUCTION

Among all the renewable energy sources, solar energy is the only candidate that can single-handedly satisfy the energy demands of modern society and can compete with non-renewable energy sources.[1,2] Solution-processable organic photovoltaics (OPVs) provide a further step toward a cheap and ecologically friendly means of solar energy conversion.[3−6] Comprehensive research efforts in chemistry,[7−9] physics, and engineering[10−13] have provided better understanding of structure–function relationships[14−16] and the working principles[10−13,17] of solution-processable OPVs, leading to a steady efficiency increase in the past decade now approaching and exceeding 10%.[2,18−25]

The efficiency of solar cells is determined primarily by the $J_{sc} \times V_{oc}$ product ($\eta = (J_{sc} \times V_{oc} \times FF)/P_{in}$, where J_{sc} is short-circuit current density, V_{oc} is open-circuit voltage,[26] FF is fill factor,[27] and P_{in} is input power in the form of solar radiation). In recent years, novel approaches have emerged with a goal to maximize the $J_{sc} \times V_{oc}$ product, while preserving the simplicity of active-layer fabrication in a single processing step. A first approach is based on the well-known donor–acceptor (D/A) method of polymer synthesis,[28] where electron-rich and

Received: September 26, 2014
Accepted: January 15, 2015
Published: January 15, 2015

DOI: 10.1021/am5066267
ACS Appl. Mater. Interfaces 2015, 7, 2322–2330

electron-poor monomer units are copolymerized to make perfectly alternating low band-gap polymers. Distinct from the classic D/A approach, where only one type of the acceptor moiety is introduced in the polymer backbone, recently novel polymer design has extended to the polymerization of at least two different acceptor units in the polymer backbone, termed two-acceptor polymers.[29,30] The possibility of incorporating multiple acceptor monomers with different strengths in the polymer backbone leads to a better control over the positions of highest occupied molecular orbital (HOMO) and lowest unoccupied molecular orbital (LUMO) energy levels,[31] which in turn determine the achievable J_{sc} and V_{oc} in organic solar cells. Furthermore, semi-random[31−33] and random[30,34−38] incorporation of multiple acceptor units in the polymer backbone allows fine-tuning of the position of energy levels of the polymers via changing the ratio between the corresponding acceptor moieties to better match the fullerene acceptor energetic in the solar cells and have better coverage of the solar spectra. For example, two-acceptor semi-random polymers containing thienopyrroledione (TPD) and diketo-pyrrolopyrrole (DPP) in the polymer backbone (P3HTT-TPD-DPP) (Figure 1) demonstrated HOMO energy levels measured

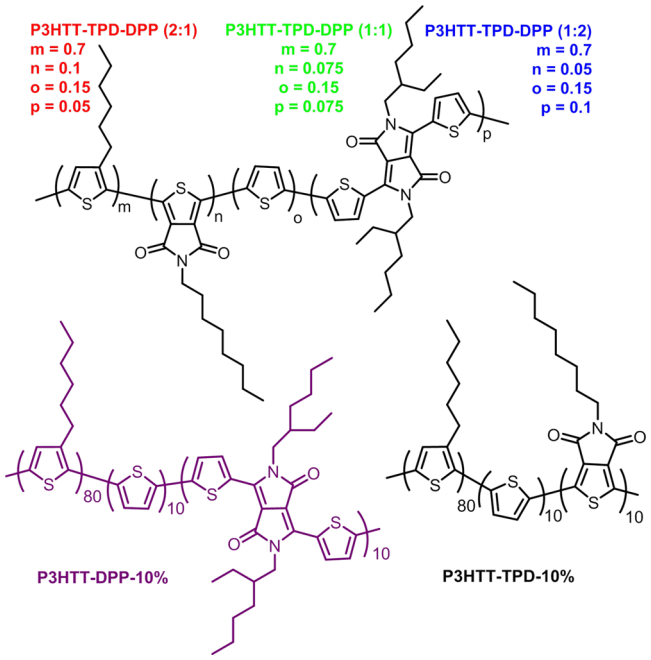

Figure 1. Structures of P3HTT-TPD-DPP (2:1), P3HTT-TPD-DPP (1:1), P3HTT-TPD-DPP (1:2), P3HTT-DPP-10%, and P3HTT-TPD-10%.

in neat polymer thin films in the range of 5.20−5.35 eV, as well as J_{sc} in the range from 11.67 mA/cm^2 to 16.37 mA/cm^2 in organic solar cells with phenyl-C_{61}-butyric acid methyl ester ($PC_{61}BM$) acceptor, based on the relative composition of the two acceptor monomers.[31]

As an alternative approach to increase the efficiency of OPVs, recently introduced ternary blend bulk heterojunction (BHJ) solar cells[39−50] have been found to enable simultaneous J_{sc} and V_{oc} increases,[40,41,49] while preserving the simplicity of the solar cell active-layer fabrication in a single processing step. The J_{sc} increase is achieved due to the spectral broadening of the photoresponse of the three-component system,[40,42,48−50] while the V_{oc} is found to be composition-dependent and tunable between the V_{oc} of the corresponding binary blend solar cells.[39−41,49,51−53] The composition-dependent electro-optical behavior of ternary blend solar cells is explained by the organic alloy model.[41,49] According to this model, extensive electronic and physical interaction of the active layer components is responsible for the formation of an "effective" LUMO or "effective" HOMO in case of the systems based on one donor and two acceptors (D1/A1/A2) or two donors and one acceptor (D1/D2/A), respectively, thus providing the continuous change in the energy of charge-transfer (CT) state[10,12,54,55] with composition and hence the V_{oc}. At the same time, individual optical transitions of all the components are preserved, explaining the possibility of simultaneous J_{sc} increase in ternary blend BHJ solar cells.

The two approaches described above have attracted significant attention due to the large variety of the polymers that can be synthesized (two-acceptor approach) and numerous polymer combinations that can be employed in the active layers of the ternary blend solar cells, even though certain restrictions should be considered for the good compatibility of the components in the three component blends.[42,56] Furthermore, the efficiency increase in each case is achieved due to two different mechanisms, specifically, careful positioning of the HOMO and LUMO energy levels of the two-acceptor polymers with respect to the fullerene acceptors in the binary blends and complementary absorption and different position of the HOMO energy levels in the case of ternary blend BHJ solar cells based on two polymers.

Of particular interest is a direct comparison of these two approaches in which the same constituent molecular components are incorporated into a solar cell, where, in one case, the components are physically mixed (ternary blend approach/organic alloy formation) and, in the other case, they are chemically "mixed", that is, covalently copolymerized (two-acceptor approach). In the present study, the electro-optical properties and device performance of ternary blend solar cells, based on two polymers containing either TPD (P3HTT-TPD-10%)[31] or DPP (P3HTT-DPP-10%)[57] in the polymer backbone (P3HTT-DPP-10%:P3HTT-TPD-10%:$PC_{61}BM$), which form an organic alloy at all studied polymer/polymer ratios, is compared with binary blend solar cells based on a series of semi-random two-acceptor polymer:$PC_{61}BM$ blends containing both DPP and TPD in the polymer backbone (P3HTT-TPD-DPP:$PC_{61}BM$),[31] as shown in Figure 1. While the optical properties and the external quantum efficiency (EQE) profiles of the binary and ternary blends were found to be similar and were described as a linear combination of the individual components, drastic differences were observed in the V_{oc} behaviors of binary and ternary blend BHJ solar cells. In case of two-acceptor polymers, the V_{oc} was found to be in the range of 0.495−0.552 V, increasing as the amount of the TPD in the polymer backbone increased. At the same time, ternary blend solar cells showed behavior inherent to organic alloy formation, with intermediate, composition-dependent, and tunable V_{oc}, as well as efficient photocurrent generation from all the components in the blend, even at very low concentrations. As a result, the V_{oc} was tuned in a wide range of values from 0.582 to 0.684 V, significantly exceeding the values achieved in the two-acceptor binary blend solar cells. Despite the differences between the physical mixing and chemical mixing approaches, the efficiencies of solar cells in both cases were found to be similar, highlighting the advantages of both pathways for enhancing the efficiency of BHJ solar cells.

DOI: 10.1021/am5066267
ACS Appl. Mater. Interfaces 2015, 7, 2322−2330

EXPERIMENTAL SECTION

Materials and Methods. All reagents from commercial sources were used without further purification, unless otherwise noted. Solvents were purchased from VWR and used without further purification except for tetrahydrofuran (THF), which was dried over sodium/benzophenone before being distilled.

For thin-film measurements, solutions were spin-coated onto precleaned glass slides from *o*-dichlorobenzene solutions at 7 mg/mL for P3HTT-DPP-10%, P3HTT-TPD-10%, P3HTT-TPD-DPP (2:1), P3HTT-TPD-DPP (1:1), and P3HTT-TPD-DPP (1:2) and at optimal ratios found for P3HTT-DPP-10%:P3HTT-TPD-10%:$PC_{61}BM$, P3HTT-TPD-DPP (2:1):$PC_{61}BM$, P3HTT-TPD-DPP (1:1):$PC_{61}BM$, and P3HTT-TPD-DPP (1:2):$PC_{61}BM$ solar cells. UV−vis absorption spectra were obtained on a PerkinElmer Lambda 950 spectrophotometer. The thickness of the thin films and grazing-incidence X-ray diffraction (GIXRD) measurements were obtained using Rigaku Diffractometer Ultima IV using Cu Kα radiation source (λ = 1.54 Å) in the reflectivity and grazing-incidence X-ray diffraction mode, respectively.

Transmission electron microscopy (TEM) was performed on the JEOL JEM-2100 microscope equipped with the Gatan Orius CCD camera. The accelerating voltage was 200 kV. Films for the TEM measurements were prepared from the *o*-dichlorobenzene solutions of P3HTT-DPP-10%:P3HTT-TPD-10%:$PC_{61}BM$ blends at the 1:0:1.3, 0.65:0.35:1.3, 0.5:0.5:1.3, 0.35:0.65:1.3, and 0:1:1.3 ratios; and P3HTT-TPD-DPP (2:1):$PC_{61}BM$ at 1:1.5 ratio, P3HTT-TPD-DPP (1:1):$PC_{61}BM$ at 1:1.7 ratio and P3HTT-TPD-DPP (1:2):$PC_{61}BM$ at 1:2.0 ratio and optimized processing conditions. Films for TEM were prepared by first spin-casting on poly(3,4-ethylenedioxythiophene) polystyrene sulfonate (PEDOT:PSS) coated glass, and they were then placed in deionized water; upon PEDOT:PSS dissolution, the floating films were picked up with the 600 hex mesh copper grid (Electron Microscopy Sciences).

Surface-energy studies of the neat polymers and fullerene derivative were performed on Ramé-Hart Instrument Co. contact angle goniometer model 290-F1 and analyzed using Surface Energy (two liquids) tool implemented in DROPimage 2.4.05 software. Prepared from the 5 mg/mL *o*-dichlorobenzene solution for P3HTT-DPP-10% and P3HTT-TPD-10% and from 5 mg/mL chloroform solution in the case of $PC_{61}BM$, the films were spin-coated on the precleaned glass slides. Water and glycerol were used as two solvents in the so-called two-liquid model to measure the contact angle, and harmonic mean Wu model[58,59] was used to calculate the average surface energy values for each film according to following set of equations:

$$\gamma_w \cdot (1 + \cos(Z^w)) = \frac{4 \cdot \gamma_w^d \cdot \gamma^d}{\gamma_w^d + \gamma^d} + \frac{4 \cdot \gamma_w^p \cdot \gamma^p}{\gamma_w^p + \gamma^p} \quad (1)$$

$$\gamma_g \cdot (1 + \cos(Z^g)) = \frac{4 \cdot \gamma_g^d \cdot \gamma^d}{\gamma_g^d + \gamma^d} + \frac{4 \cdot \gamma_g^p \cdot \gamma^p}{\gamma_g^p + \gamma^p} \quad (2)$$

$$\gamma^{tot} = \gamma^d + \gamma^p \quad (3)$$

$$\gamma_w = 72.8 mJ/m^2;\ \gamma_w^d = 21.8 mJ/m^2;\ \gamma_w^p = 51.0 mJ/m^2$$

$$\gamma_g = 64.0 mJ/m^2;\ \gamma_g^d = 34.0 mJ/m^2;\ \gamma_g^p = 30.0 mJ/m^2$$

where Z^w is the contact angle with water, Z^g is the contact angle with glycerol, γ^{tot} is the total surface energy, γ^p and γ^d are polar and dispersive surface energy components.

Synthetic Procedures. Synthetic procedures for the synthesis of poly(3-hexylthiophene-thiophene-diketopyrrolopyrrole) (P3HTT-DPP-10%) (Mn = 20,500, PDI = 2.60), poly(3-hexylthiophene-thiophene-thienopyrroledione) (P3HTT-TPD-10%) (Mn = 22,630, PDI = 1.98), poly(3-hexylthiophene-thiophene-thienopyrroledione-diketopyrrolopyrrole) (P3HTT-TPD-DPP (2:1) (Mn = 12,650, PDI = 3.36), P3HTT-TPD-DPP (1:1) (Mn = 11,730, PDI = 2.98) and P3HTT-TPD-DPP (1:2) (Mn = 19,700, PDI = 3.07)) were used without modifications as reported in the literature.[31,57]

Device Fabrication and Characterization. All steps of device fabrication and testing were performed in air. ITO-coated glass substrates (10 $\Omega/\square^2$, Thin Film Devices Inc.) were sequentially cleaned by sonication in detergent, deionized water, tetrachloroethylene, acetone, and isopropyl alcohol and dried in a nitrogen stream. A thin layer of PEDOT:PSS (Clevios PH500, filtered with a 0.45 μm poly(vinylidene fluoride) syringe filter—Pall Life Sciences) was first spin-coated on the precleaned ITO-coated glass substrates and baked at 130 °C for 60 min under vacuum. Separate solutions of P3HTT-DPP-10%, P3HTT-TPD-10%, and $PC_{61}BM$ were prepared in *o*-dichlorobenzene solvent. The solutions were stirred for 24 h before they were mixed at the desired ratios and stirred for 24 h to form a homogeneous mixture. Subsequently, the P3HTT-DPP-10%:P3HTT-TPD-10%:$PC_{61}BM$ active layer was spin-coated (with a 0.45 μm polytetrafluoroethylene syringe filter—Pall Life Sciences) on top of the PEDOT:PSS layer. Concentrations of the binary and ternary blends were 10 mg/mL in polymer or P3HTT-DPP-10%:P3HTT-TPD-10%. Upon spin-coating of P3HTT-DPP-10%:P3HTT-TPD-10%:$PC_{61}BM$, films were first placed in the N_2 cabinet for 30 min and then placed in the vacuum chamber for aluminum deposition. At the final stage, the substrates were exposed to high vacuum ($<9 \times 10^{-7}$ Torr), and aluminum (100 nm) was thermally evaporated at 3−4 Å/s using a Denton Benchtop Turbo IV Coating System onto the active layer through shadow masks to define the active area of the devices as 4.4 mm^2.

The current−voltage (I−V) characteristics of the photovoltaic devices were measured under ambient conditions using a Keithley 2400 source-measurement unit. An Oriel Sol3A class AAA solar simulator with xenon lamp (450 W) and an AM 1.5G filter was used as the solar simulator. An Oriel PV reference cell system 91150 V was used as the reference cell. To calibrate the light intensity of the solar simulator (to 100 mW/cm^2), the power of the xenon lamp was adjusted to make the short-circuit current density (J_{sc}) of the reference cell under simulated sun light as high as it was under the calibration condition.

The EQE measurements were performed using a 300 W xenon arc lamp (Newport Oriel), chopped and filtered monochromatic light (250 Hz, 10 nm fwhm) from a Conerstone 260 1/4 M double grating monochromator (Newport 74125) together with a light-bias lock-in amplifier. A silicon photodiode calibrated at Newport was utilized as the reference cell.

Mobility was measured using a hole-only device configuration of ITO/PEDOT:PSS/P3HTT-DPP-10%:P3HTT-TPD-10%:$PC_{61}BM$/Al or ITO/PEDOT:PSS/P3HTT-TPD-DPP:$PC_{61}BM$/Al in the space charge limited current regime as described elsewhere.[60] The device preparation for a hole-only device was the same as that described above for solar cells. The dark current was measured under ambient conditions.

RESULTS AND DISCUSSION

Recently, we reported a family of semi-random two-acceptor polymers (P3HTT-TPD-DPP), where the ratio between the acceptor moieties TPD and DPP in the polymer backbone was varied from 2:1 to 1:1 and 1:2 all at an overall acceptor content of 15%,[31] as shown in Figure 1. The choice of the acceptor units was influenced by the ability of TPD to lower the position of the HOMO energy level and the known high efficiency of semi-random polymers containing DPP in the binary blends BHJ solar cells with a $PC_{61}BM$ acceptor.[31,57] P3HTT-TPD-DPP polymers showed strong and uniform absorption in the visible and near-IR (Figure 2), and the absorption profiles were found to be linear combinations of the absorption profiles of the polymers containing only one acceptor in the polymer backbone, P3HTT-TPD-10% and P3HTT-DPP-10%, respectively. As a result of the uniformly strong absorption, high photoresponses of the polymer:$PC_{61}BM$ solar cells in the 350−

DOI: 10.1021/am5066267
ACS Appl. Mater. Interfaces 2015, 7, 2322−2330

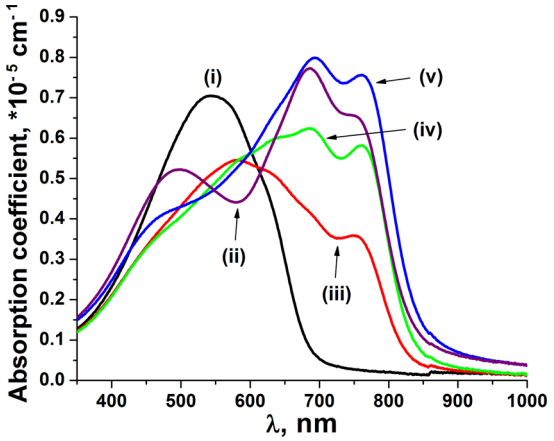

Figure 2. Absorption profiles of neat polymers in thin films. (i) P3HTT-TPD-10%. (ii) P3HTT-DPP-10%. (iii) P3HTT-TPD-DPP (2:1). (iv) P3HTT-TPD-DPP (1:1). (v) P3HTT-TPD-DPP (1:2).

850 nm range were recorded and translated into high J_{sc} exceeding 16 mA/cm^2 for the case of P3HTT-TPD-DPP (1:2):PC$_{61}$BM, as can be seen in Table 1. Consequently,

Table 1. Photovoltaic Properties of Ternary Blend P3HTT-DPP-10%:P3HTT-TPD-10%:PC$_{61}$BM and Binary Blend P3HTT-TPD-DPP:PC$_{61}$BM BHJ Solar Cells

P3HTT-DPP-10%:P3HTT-TPD-10%:PC$_{61}$BM[a]	J_{sc} (mA/cm^2)[b,c]	V_{oc} (V)[d]	FF[e]	η (%)[f]
1:0:1.3	14.45	0.582	0.63	5.27
0.9:0.1:1.3	13.61	0.596	0.63	5.01
0.8:0.2:1.3	11.96	0.605	0.63	4.55
0.65:0.35:1.3	11.06	0.613	0.64	4.32
0.5:0.5:1.3	9.03	0.620	0.60	3.28
0.35:0.65:1.3	8.17	0.630	0.59	3.06
0.2:0.8:1.3	6.59	0.634	0.59	2.45
0.1:0.9:1.3	5.77	0.644	0.59	2.12
0.07:0.93:1.3	5.35	0.645	0.60	1.98
0.03:0.97:1.3	5.27	0.663	0.61	2.13
0:1:1.3	4.92	0.684	0.64	2.15
P3HTT-TPD-DPP (2:1)[g]	11.67	0.552	0.62	3.94
P3HTT-TPD-DPP (1:1)[g]	15.26	0.509	0.64	4.93
P3HTT-TPD-DPP (1:2)[g]	16.37	0.495	0.61	4.92

[a]All devices were spin-coated from *o*-dichlorobenzene (*o*-DCB) and dried under N_2 for 30 min before aluminum deposition. [b]Mismatch corrected. [c]Standard deviations of less than 0.5 mA/cm^2 were observed in all cases averaged over eight pixels. [d]Standard deviations of less than 0.005 V were observed in all cases averaged over eight pixels. [e]Standard deviations of less than 0.02 were observed in all cases averaged over eight pixels. [f]Standard deviations of less than 0.2% were observed in all cases averaged over eight pixels. [g]From ref 31.

efficiencies approaching 5% were achieved for the P3HTT-TPD-DPP:PC$_{61}$BM solar cells. Further efficiency increase was limited by the moderate V_{oc} in the range of 0.50−0.55 V.

To overcome the V_{oc} limitation found in P3HTT-TPD-DPP:PC$_{61}$BM solar cells and compare the electro-optical properties and solar cell performances between the physical mixing and chemical mixing of the components, we studied the ternary blend system based on polymer donors containing either DPP or TPD in the polymer backbone, with PC$_{61}$BM acceptor. As discussed earlier, the absorption profiles of P3HTT-TPD-DPP polymers were found to be a linear combination of the complementary absorption profiles of low band-gap P3HTT-DPP-10% and large band-gap P3HTT-TPD-10%, thus making these two polymers excellent candidates for complementary absorption and the exploration of the individual contribution of the polymers in the photocurrent generation in ternary blends. Additionally, HOMO energy levels of P3HTT-DPP-10% and P3HTT-TPD-10%, measured in thin films, are significantly different (5.2 eV vs 5.4 eV, respectively),[31] consequently allowing a composition-dependent V_{oc} based on the ratio of the donor polymers. Since organic alloy formation between synergistic components is rooted in a strong physical interaction between the components, the semi-random nature of both polymers, which both contain 80% of 3-hexylthiophene repeat units, should provide good miscibility in the polymer pair as supported by the random-copolymer effect,[61,62] commonly used to engender miscibility between polymers through the random incorporation of common comonomers. Additionally, similar surface energies of 19.9 and 20.7 mN/m for P3HTT-DPP-10% and P3HTT-TPD-10%, respectively, support good miscibility between the polymers, and surface energy has proven an effective predictor of BHJ morphology.[42,59,63−65]

Photovoltaic devices containing ternary blends in a conventional device configuration of ITO/PEDOT:PSS/P3HTT-DPP-10%:P3HTT-TPD-10%:PC$_{61}$BM/Al were fabricated in air. Binary blend solar cells with both polymers showed optimal device performance at donor:PC$_{61}$BM ratio of 1:1.3 under the same processing conditions. As a result, in the case of ternary blend solar cells the overall polymer:fullerene ratio was kept constant at 1:1.3, while the ratio between P3HTT-DPP-10% and P3HTT-TPD-10% was varied from 1:0 to 0:1. Film thicknesses were kept constant at 85−90 nm, for the direct comparison to P3HTT-TPD-DPP:PC$_{61}$BM solar cells. Table 1 lists the average values of J_{sc}, V_{oc}, FF, and η obtained under simulated AM 1.5G illumination (100 mW/cm^2).

As can be seen in Table 1, the V_{oc} of the ternary blend P3HTT-DPP-10%:P3HTT-TPD-10%:PC$_{61}$BM solar cells increases, as the amount of the P3HTT-TPD-10% with deeper-lying HOMO energy level in the three component system increases. The observed V_{oc} behavior in the ternary blend regime is consistent with the organic alloy model, where strong physical and electronic interaction between the components in the blends leads to the formation of an effective HOMO energy level, which varies with changes in the composition of the three component blend. If the compatibility between the components would be low, we should expect pinning of the smallest V_{oc} of corresponding binary blend solar cells. Furthermore, as in the previously studied ternary blend system based on poly(3-hexylthiophene-*co*-3-(2-ethylhexyl)thiophene) (P3HT$_{75}$-*co*-EHT$_{25}$) and P3HTT-DPP-10%,[40] the V_{oc} behavior in the ternary blend regime was found to change linearly in the range from 0.9:0.1:1.3 to 0.07:0.93:1.3, as can be seen in Figure 3a. Upon further increase of the P3HTT-TPD-10% content in the ternary blend, the V_{oc} behavior deviates from linearity. This result implies that the V_{oc}, and hence the energy of the CT state in the ternary blend solar cells, is extremely sensitive to the composition, and even small contents are sufficient to effectively alter the V_{oc}.

Unlike the V_{oc} increase, J_{sc} was found to decrease in a linear fashion with the increase of P3HTT-TPD-10% content in the three-component blends for the films of the same thicknesses, as shown in Figure 3a. However, even at small P3HTT-DPP-10% ratios (below 10%), the J_{sc} of the ternary blends is higher

DOI: 10.1021/am5066267
ACS Appl. Mater. Interfaces 2015, 7, 2322−2330

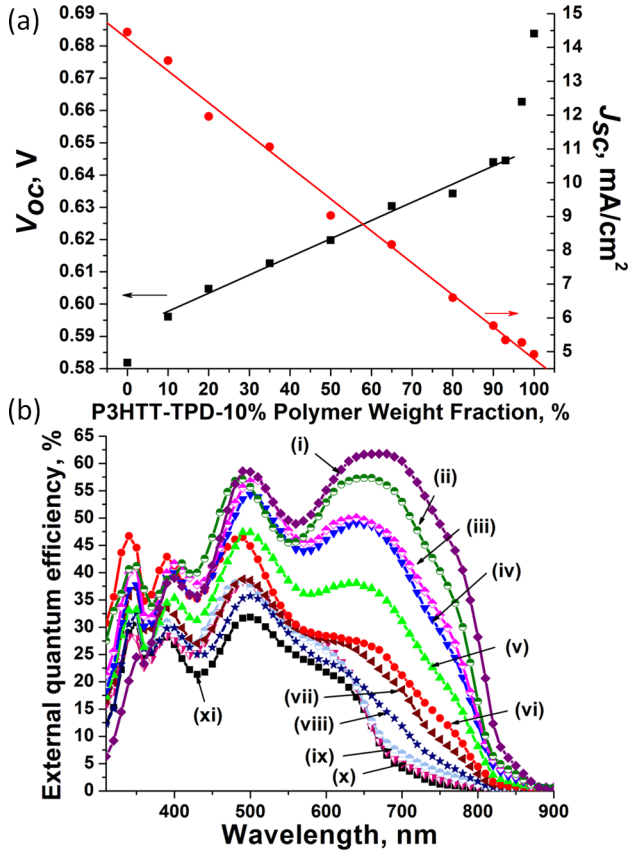

Figure 3. (a) Open-circuit voltage (black squares, left axis) and short-circuit current density (J_{sc}) (red circles, right axis) of the ternary blend BHJ solar cells as a function of the amount of P3HTT-TPD-10% in the blends. (b) External quantum efficiency of ternary blend BHJ solar cells. (i) 1:0:1.3 (purple line). (ii) 0.9:0.1:1.3 (olive line). (iii) 0.8:0.2:1.3 (magenta line). (iv) 0.65:0.35:1.3 (blue line). (v) 0.5:0.5:1.3 (green line). (vi) 0.35:0.65:1.3 (red line). (vii) 0.2:0.8:1.3 (wine-red line). (viii) 0.1:0.9:1.3 (navy line). (ix) 0.07:0.93:1.3 (cyan line). (x) 0.03:0.97:1.3 (pink line). (xi) 0:1:1.3 (black line).

than that of P3HTT-TPD-10%:$PC_{61}BM$ binary blends. This behavior is explained based on the complementary absorption profiles of P3HTT-DPP-10% and P3HTT-TPD-10% (Figure 2). The increase of the P3HTT-DPP-10% content in the three component blends leads to the enhancement of light absorption in the near-IR and hence increases the number of photons absorbed (see Supporting Information). Moreover, as in previously studied systems, where either both polymers were semicrystalline (P3HTT-DPP-10%:$P3HT_{75}$-*co*-EHT_{25}:$PC_{61}BM$)[40] or only one polymer was semicrystalline (P3HTT-DPP-10%:PCDTBT:$PC_{61}BM$, where PCDTBT is poly[*N*-9′-heptadecanyl-2,7-carbazole-*alt*-5,5-(4′,7′-di-2-thienyl-2′,1′,3′-benzothiadiazole)]—amorphous),[42] the position of the long-wavelength peak does not change with composition and only changes intensity, while the high-energy-region peak red-shifts with the increase of the P3HTT-TPD-10%. The overall J_{sc} decrease observed with the increase of the P3HTT-TPD-10% content is attributed to the continuous decrease of the light absorption by the P3HTT-DPP-10% chromophore (near-IR), even though light absorption in the 300–600 nm range is enhanced.

The EQE measurements were performed to further investigate the origin of the J_{sc} changes. The measured photoresponse from the ternary blends, as shown in Figure 3b, correlates well with the complementary absorption profiles from both polymers obtained by UV–vis. P3HTT-TPD-10%:$PC_{61}BM$ has a strong photoresponse across the visible part of the solar spectrum. The incorporation of the P3HTT-DPP-10% in the three-component blend leads to significant enhancement of the EQE values not only in the near-IR, but in the visible region as well. As a result, the number of the photons that can contribute to the photocurrent increases, leading to the observed J_{sc} enhancement. It is important to mention that photoresponse from the low band-gap P3HTT-DPP-10% in the ternary blend is already observed at only 3% ratio (0.03:0.97:1.3) (see Supporting Information), implying that excitons created in this dilute component effectively reach the interface and split into electron–hole pairs, with the same efficiency as they do at high concentrations.

High FF values, exceeding 0.59, were obtained for all ternary blend compositions. This can be attributed to the preservation of the semicrystalline nature of P3HTT-DPP-10% in the ternary blends, balanced, trap-free charge transport through the bulk and favorable morphology.[27,66−68] Even though P3HTT-TPD-10% was found to be amorphous in neat and binary blends, P3HTT-DPP-10% retains its semicrystalline nature as can be seen from the presence of the vibronic shoulder in the UV–vis spectra, as well as the presence of the peak in the GIXRD data for binary and ternary blends (see Supporting Information). Furthermore, the interchain distance in the (100) direction decreases with the increase of the P3HTT-DPP-10% content in the three-component blends, allowing tighter packing of the polymer chains, thus contributing to high J_{sc} and FF. The ability of P3HTT-DPP-10% to retain semicrystallinity in the blends translates into high hole mobilities, in the range from 2.09×10^{-3} to 2.70×10^{-3} cm^2 V^{-1} s^{-1}, measured in binary and ternary blend solar cells, preventing space-charge buildup and population of deep traps (see Supporting Information).[68] The TEM images (see Supporting Information) show similar bicontinuous blends with nanometer-scale phase separation at different P3HTT-DPP-10%:P3HTT-TPD-10%:$PC_{61}BM$ ratios.

The combination of the intermediate and composition-dependent V_{oc}, even at 0.03:0.97:1.3 ratio, preservation of the individual excitonic properties of all the components observed in the UV–vis spectra, excellent correlation between UV–vis and EQE spectra (Figure 3), high FF values at all ternary blend compositions, as well as similar surface energies of the P3HTT-DPP-10% and P3HTT-TPD-10% polymers support the formation of organic alloys in the case of P3HTT-DPP-10%:P3HTT-TPD-10%:$PC_{61}BM$ ternary blend solar cells. Furthermore, evidence of exciton traps was not observed in the P3HTT-DPP-10%:P3HTT-TPD-10%:$PC_{61}BM$ system at any ratio and efficient exciton contribution to the photocurrent at low doping ratios of low band-gap P3HTT-DPP-10% was recorded. This is in strong contrast to the formation of an exciton trap on P3HTT-DPP-10% observed in the non-alloy-forming P3HTT-DPP-10%:PCDTBT:$PC_{61}BM$ ternary blends at small (≤60%) P3HTT-DPP-10% concentrations.[42]

As a result of organic alloy formation in the case of P3HTT-DPP-10%:P3HTT-TPD-10%:$PC_{61}BM$ ternary blend solar cells, high FF, as well as preservation of important individual properties of the donor polymers in the three component blends, power conversion efficiencies of the ternary blend solar cells were found to be higher than that of the P3HTT-TPD-10%:$PC_{61}BM$ binary blend solar cells at P3HTT-DPP-10% loadings exceeding 10%. However, since the film thicknesses of

DOI: 10.1021/am5066267
ACS Appl. Mater. Interfaces 2015, 7, 2322−2330

all solar cells were kept constant, the efficiency of ternary blend solar cells did not exceed that of the P3HTT-DPP-10%:$PC_{61}BM$.

The efficiencies obtained using ternary blends based on two donor polymers, namely, P3HTT-DPP-10% and P3HTT-TPD-10%, are similar to those of the binary blends containing the same acceptor monomer units in the polymer backbone (P3HTT-TPD-DPP), despite significant discrepancies in the obtained V_{oc} for the two approaches. However, high efficiencies in both cases are achieved via the two different pathways. In the case of ternary blend solar cells, the formation of an organic alloy, which leads to the tunable and composition-dependent V_{oc} as well as J_{sc}, is responsible for efficiencies approaching 5%. At the same time, P3HTT-TPD-DPP:$PC_{61}BM$ solar cells with different ratios between TPD and DPP moieties in the polymer backbone reach very high J_{sc}, exceeding 16 mA/cm^2 for P3HTT-TPD-DPP (1:2):$PC_{61}BM$, but an expense of moderate V_{oc}.

Further comparison of the electro-optical properties of P3HTT-TPD-DPP:$PC_{61}BM$ and P3HTT-DPP-10%:P3HTT-TPD-10%:$PC_{61}BM$ blends revealed additional similarities between the studied blends. In the case of thin-film UV−vis absorption of the blends, the absorption profiles of P3HTT-TPD-DPP:$PC_{61}BM$ binary blends with TPD:DPP ratios of 2:1, 1:1, and 1:2 were compared with the closest matching analogous ternary blends with DPP:TPD ratios of 0.65:0.35, 0.5:0.5, and 0.35:0.65, as seen in Figure 4a. It is observed that similar features, such as strong absorption across the visible and near-IR spectral regions, as well as presence of the vibronic shoulder at ∼750 nm in all cases. Moreover, the peak positions corresponding to the DPP chromophore and the vibronic shoulder with the similar absorption intensities in case of binary and ternary blends, which are present at ∼680 and 760 nm, respectively, do not shift as the ratio between P3HTT-DPP-10% and P3HTT-TPD-10% or DPP and TPD acceptor moieties in the two-acceptor polymer backbones changes (see Supporting Information). At the same time, P3HTT-TPD-DPP:$PC_{61}BM$ blends lack a pronounced absorption peak in the visible, while strong absorption by the P3HTT-TPD-10% polymer in the visible is observed at all studied ratios for the ternary blends, with the peak position red-shifting and intensity increasing as the amount of P3HTT-DPP-10% in the three-component blend decreases.

The similarities in the UV−vis absorption profiles for the P3HTT-TPD-DPP:$PC_{61}BM$ and P3HTT-DPP-10%:P3HTT-TPD-10%:$PC_{61}BM$ blends at similar ratios between the DPP and TPD monomer units translate into similar EQE traces, as shown in Figure 4b, highlighting the high efficiency of the photon-to-electron conversion in both systems. Even though the shapes of the EQE responses closely follow the shapes of the absorption profiles of the blends, the EQE values of the P3HTT-TPD-DPP:$PC_{61}BM$ solar cells exceed those of the ternary blend solar cells, especially in the near-IR. This discrepancy is based on the fact that the film thickness of all studied films was kept constant at 85−90 nm, thus diluting the P3HTT-DPP-10% chromophore responsible for the photon absorption in the visible and especially in the near-IR for the ternary blend BHJ solar cells. As a result, the photoresponse of the ternary blend solar cells is found to be smaller than that of P3HTT-TPD-DPP:$PC_{61}BM$ binary blend solar cells, explaining the smaller values of the obtained J_{sc}. It is interesting to note that line iii (P3HTT-DPP-10%:P3HTT-TPD-10%:$PC_{61}BM$ (0.65:0.35:1.3)) and line iv (P3HTT-TPD-DPP (2:1)) overlay

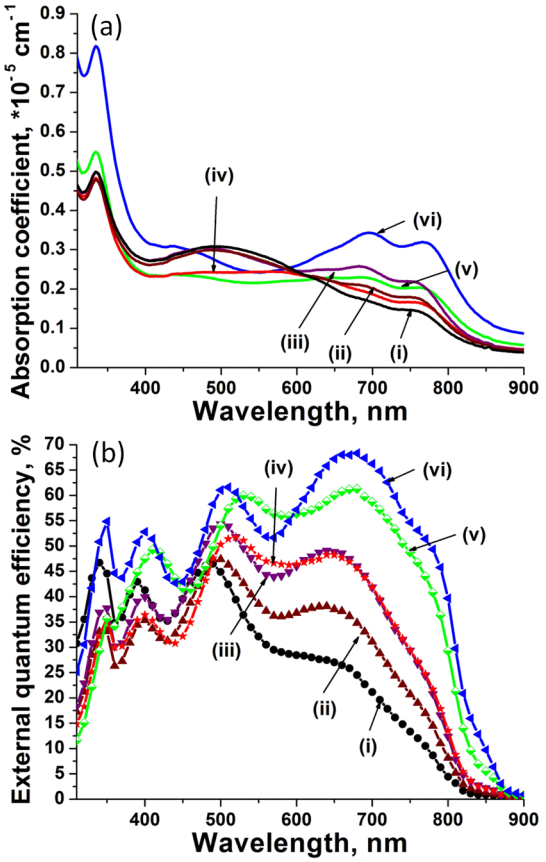

Figure 4. (a) Absorption profiles and (b) external quantum efficiency of ternary blend BHJ solar cells P3HTT-DPP-10%:P3HTT-TPD-10%:$PC_{61}BM$ where (i) is 0.35:0.65:1.3 (black line), (ii) is 0.5:0.5:1.3 (wine-red line), and (iii) is 0.65:0.35:1.3 (purple line) and binary blends where (iv) is P3HTT-TPD-DPP (2:1) (red line), (v) is P3HTT-TPD-DPP (1:1) (green line), and (vi) is P3HTT-TPD-DPP (1:2) (blue line).

almost perfectly, reflecting the similarity of the optical properties of these blends based on the same molecular components.

Unlike the similarities in the UV−vis and hence the EQE for P3HTT-TPD-DPP:$PC_{61}BM$ and P3HTT-DPP-10%:P3HTT-TPD-10%:$PC_{61}BM$ solar cells, the V_{oc} was determined to differ substantially in the two studied systems. In the case of the P3HTT-TPD-DPP:$PC_{61}BM$ solar cells, the V_{oc} was limited in the range of 0.495−0.552 V, depending on the ratio between TPD and DPP in the polymer backbone. For the ternary blend solar cells, the ability of the components to form an organic alloy allowed effective tuning of the V_{oc} in the range determined by the corresponding binary blend solar cells of P3HTT-DPP-10%:$PC_{61}BM$ and P3HTT-TPD-10%:$PC_{61}BM$ of 0.582 and 0.684 V, respectively. As such, a gain in V_{oc} of 50−150 V is achieved for the P3HTT-DPP-10%:P3HTT-TPD-10%:$PC_{61}BM$ ternary blend solar cells with respect to the P3HTT-TPD-DPP:$PC_{61}BM$ binary blend solar cells, providing an important avenue toward high efficiencies.

A direct comparison of the photovoltaic performance between the different types of blends with similar molecular composition is seen by examining Table 1. Specifically, the two-acceptor polymer P3HTT-TPD-DPP (1:1) with a 1:1 TPD:DPP ratio is compared to the ternary blend 0.5:0.5:1.3 which also has a 1:1 TPD:DPP ratio. Here the V_{oc} is increased

DOI: 10.1021/am5066267
ACS Appl. Mater. Interfaces 2015, 7, 2322−2330

by over 100 mV from 0.509 to 0.620 V in the ternary blend, and in both cases FF ≥ 0.6. However, in the ternary blend the J_{sc} is significantly lower at 9.03 mA/cm^2 as compared to 15.26 mA/cm^2 in the binary case. This is a reflection of the constant film thickness as described previously. This comparison offers a clear perspective of the contrasting merits of the two approaches. Moving to thicker films with the ternary blends could potentially result in increased J_{sc} (approaching the two-acceptor polymer case),[69] but the intrinsic V_{oc} limitation of the binary approach is evident.

The morphology comparison of the binary and ternary blend thin films using GIXRD (see Supporting Information) does not demonstrate significant differences and proves the ability of polymers to retain their semicrystalline nature in blends with $PC_{61}BM$. These data are consistent with the presence of the vibronic shoulder observed in the UV−vis in all studied cases for the thin film blends with fullerene acceptor. Furthermore, the interchain distances in the (100) direction for binary and ternary blend thin films are found to be similar in the range of 15.6−16.4 Å, contributing to the high J_{sc} obtained.

High and similar FFs in the range of 0.59−0.64 were achieved in all studied binary and ternary blend solar-cell systems. This can be attributed to the formation of favorable morphology and efficient charge transport in the solar cells.[27,66−68] As seen in the TEM images (see Supporting Information), P3HTT-TPD-DPP:$PC_{61}BM$ and P3HTT-DPP-10%:P3HTT-TPD-10%:$PC_{61}BM$ blends all form similar bicontinuous blends with a nanometer-scale phase separation at all compositions. Thus, introduction of the third component in case of the ternary blend solar cells does not lead to significant changes in the morphology, and excitons can effectively reach the D/A interface and dissociate into free charge carriers, which can subsequently be transported through the interpenetrated network to the corresponding contacts, as in case of P3HTT-TPD-DPP:$PC_{61}BM$ binary blends. The formation of favorable morphology, as well as the preservation of the semicrystalline nature of polymers in binary and ternary blends translated into high hole mobilities ∼2 × 10^{-3} cm^2 V^{-1} s^{-1} measured in the space-charge limited current regime for P3HTT-TPD-DPP:$PC_{61}BM$ and P3HTT-DPP-10%:P3HTT-TPD-10%:$PC_{61}BM$ blends. As a result, no charge trapping or space-charge buildup is observed in any of the studied systems.[68]

SUMMARY AND CONCLUSION

In the present work, we studied the effect of incorporating the same constituent molecular components into a solar cell, where in one case the components form an organic alloy in ternary blends (physically mixed) and in the other case units are covalently copolymerized to form two-acceptor polymers (chemically mixed). Solar cells based on the two-acceptor polymers and ternary blends showed similar electro-optical and morphological properties, which translated into high J_{sc}, FF, and efficiencies. However, the V_{oc} behavior was drastically different. In case of ternary blends, which formed an organic alloy, the V_{oc} was found to be composition-dependent and tunable, while the two-acceptor polymer solar cells had similar V_{oc} values, which was 50−150 mV lower than that of ternary blend solar cells with the same composition. Interestingly, even at low concentrations of the third components (<10%) in the ternary blends, the V_{oc} was found to be extremely sensitive and tunable with composition. Furthermore, photons absorbed by the diluted third components were able to effectively contribute to the photocurrent, demonstrating the significant effect of all the ternary components on the solar-cell performance. The current study provides further motivation for the necessity of the research in the field of ternary blend BHJ solar cells and two-acceptor polymers. Clearly, both approaches have important advantages for efficient solar cells manufactured in a single active-layer processing step.

ASSOCIATED CONTENT

Supporting Information

Solar cell fabrication procedures, spectral mismatch correction, surface energy, GIXRD, UV−vis, EQE, TEM, XRD, mobility, and J−V data. This material is available free of charge via the Internet at http://pubs.acs.org.

AUTHOR INFORMATION

Corresponding Author

*E-mail: barrycth@usc.edu.

Author Contributions

The manuscript was written through contributions of all authors. All authors have given approval to the final version of the manuscript.

Notes

The authors declare no competing financial interest.

ACKNOWLEDGMENTS

This material is based upon work supported as part of the Center for Energy Nanoscience, an Energy Frontier Research Center funded by U.S. Department of Energy, Office of Science, Office of Basic Energy Sciences under Award No. DE-SC0001013 for partial support of P.P.K, A.E.R, B.B., and B.C.T. Funding from the National Science Foundation (CBET Energy for Sustainability) CBET-1436875 is also acknowledged. We also thank Prof. M. Gupta for use of a contact angle goniometer.

REFERENCES

(1) Armaroli, N.; Balzani, V. Towards an Electricity-Powered World. *Energy Environ. Sci.* **2011**, *4*, 3193−3222.

(2) Ameri, T.; Li, N.; Brabec, C. J. Highly Efficient Organic Tandem Solar Cells: A Follow up Review. *Energy Environ. Sci.* **2013**, *6*, 2390−2413.

(3) Yan, J.; Saunders, B. R. Third-generation Solar Cells: A Review and Comparison of Polymer:Fullerene, Hybrid Polymer and Perovskite Solar Cells. *RSC Adv.* **2014**, *4*, 43286−43314.

(4) Mazzio, K. A.; Luscombe, C. K. The Future of Organic Photovoltaics. *Chem. Soc. Rev.* **2014**, DOI: 10.1039/C4CS00227J.

(5) Dou, L.; You, J.; Hong, Z.; Xu, Z.; Li, G.; Street, R. A.; Yang, Y. 25th Anniversary Article: A Decade of Organic/Polymeric Photovoltaic Research. *Adv. Mater.* **2013**, *25*, 6642−6671.

(6) Thompson, B. C.; Khlyabich, P. P.; Burkhart, B.; Aviles, A. E.; Rudenko, A.; Shultz, G. V.; Ng, C. F.; Mangubat, L. B. Polymer-Based Solar Cells: State-of-the-Art Principles for the Design of Active Layer Components. *Green* **2011**, *1*, 29−54.

(7) Marzano, G.; Ciasca, C. V.; Babudri, F.; Bianchi, G.; Pellegrino, A.; Po, R.; Farinola, G. M. Organometallic Approaches to Conjugated Polymers for Plastic Solar Cells: From Laboratory Synthesis to Industrial Production: Organometallic Approaches to Polymers for Plastic Solar Cells. *Eur. J. Org. Chem.* **2014**, *30*, 6583−6614.

(8) Burke, D. J.; Lipomi, D. J. Green Chemistry for Organic Solar Cells. *Energy Environ. Sci.* **2013**, *6*, 2053−2066.

(9) Carsten, B.; He, F.; Son, H. J.; Xu, T.; Yu, L. Stille Polycondensation for Synthesis of Functional Materials. *Chem. Rev.* **2011**, *111*, 1493−1528.

DOI: 10.1021/am5066267
ACS Appl. Mater. Interfaces 2015, 7, 2322−2330

(10) Deibel, C. Photocurrent Generation in Organic Solar Cells. *Semicond. Semimetals* **2011**, *85*, 297.
(11) Deibel, C.; Dyakonov, V. Polymer−Fullerene Bulk Heterojunction Solar Cells. *Rep. Prog. Phys.* **2010**, *73*, 096401.
(12) Clarke, T. M.; Durrant, J. R. Charge Photogeneration in Organic Solar Cells. *Chem. Rev.* **2010**, *110*, 6736−6767.
(13) Gao, F.; Inganäs, O. Charge Generation in Polymer−Fullerene Bulk-Heterojunction Solar Cells. *Phys. Chem. Chem. Phys.* **2014**, *16*, 20291−20304.
(14) Zhou, H.; Yang, L.; You, W. Rational Design of High Performance Conjugated Polymers for Organic Solar Cells. *Macromolecules* **2012**, *45*, 607−632.
(15) Chochos, C. L.; Choulis, S. A. How the Structural Deviations on the Backbone of Conjugated Polymers Influence Their Optoelectronic Properties and Photovoltaic Performance. *Prog. Polym. Sci.* **2011**, *36*, 1326−1414.
(16) Uy, R. L.; Price, S. C.; You, W. Structure-Property Optimizations in Donor Polymers via Electronics, Substituents, and Side Chains Toward High Efficiency Solar Cells. *Macromol. Rapid Commun.* **2012**, *33*, 1162−1177.
(17) Brédas, J.-L.; Norton, J. E.; Cornil, J.; Coropceanu, V. Molecular Understanding of Organic Solar Cells: The Challenges. *Acc. Chem. Res.* **2009**, *42*, 1691−1699.
(18) Li, W.; Furlan, A.; Hendriks, K. H.; Wienk, M. M.; Janssen, R. A. J. Efficient Tandem and Triple-Junction Polymer Solar Cells. *J. Am. Chem. Soc.* **2013**, *135*, 5529−5532.
(19) You, J.; Dou, L.; Yoshimura, K.; Kato, T.; Ohya, K.; Moriarty, T.; Emery, K.; Chen, C.-C.; Gao, J.; Li, G.; Yang, Y. A Polymer Tandem Solar Cell with 10.6% Power Conversion Efficiency. *Nat. Commun.* **2013**, *4*, 1446.
(20) You, J.; Chen, C.-C.; Hong, Z.; Yoshimura, K.; Ohya, K.; Xu, R.; Ye, S.; Gao, J.; Li, G.; Yang, Y. 10.2% Power Conversion Efficiency Polymer Tandem Solar Cells Consisting of Two Identical Sub-Cells. *Adv. Mater.* **2013**, *25*, 3973−3978.
(21) Liu, Y.; Chen, C.-C.; Hong, Z.; Gao, J.; (Michael) Yang, Y.; Zhou, H.; Dou, L.; Li, G.; Yang, Y. Solution-Processed Small-Molecule Solar Cells: Breaking the 10% Power Conversion Efficiency. *Sci. Rep.* **2013**, *3*, 3356.
(22) Zhang, K.; Zhong, C.; Liu, S.; Mu, C.; Li, Z.; Yan, H.; Huang, F.; Cao, Y. Highly Efficient Inverted Polymer Solar Cells Based on a Cross-Linkable Water-/Alcohol-Soluble Conjugated Polymer Interlayer. *ACS Appl. Mater. Interfaces* **2014**, *6*, 10429−10435.
(23) Elshobaki, M.; Anderegg, J.; Chaudhary, S. Efficient Polymer Solar Cells Fabricated on Poly(3,4-ethylenedioxythiophene):Poly-(styrenesulfonate)-Etched Old Indium Tin Oxide Substrates. *ACS Appl. Mater. Interfaces* **2014**, *6*, 12196−12202.
(24) Li, C.-Z.; Chang, C.-Y.; Zang, Y.; Ju, H.-X.; Chueh, C.-C.; Liang, P.-W.; Cho, N.; Ginger, D. S.; Jen, A. K.-Y. Suppressed Charge Recombination in Inverted Organic Photovoltaics via Enhanced Charge Extraction by Using a Conductive Fullerene Electron Transport Layer. *Adv. Mater.* **2014**, *26*, 6262−6267.
(25) Chen, C.-C.; Chang, W.-H.; Yoshimura, K.; Ohya, K.; You, J.; Gao, J.; Hong, Z.; Yang, Y. An Efficient Triple-Junction Polymer Solar Cell Having a Power Conversion Efficiency Exceeding 11%. *Adv. Mater.* **2014**, *26*, 5670−5677.
(26) Qi, B.; Wang, J. Open-circuit Voltage in Organic Solar Cells. *J. Mater. Chem.* **2012**, *22*, 24315−24325.
(27) Qi, B.; Wang, J. Fill Factor in Organic Solar Cells. *Phys. Chem. Chem. Phys.* **2013**, *15*, 8972−8982.
(28) Bundgaard, E.; Krebs, F. Low Band Gap Polymers for Organic Photovoltaics. *Sol. Energy Mater. Sol. Cells* **2007**, *91*, 954−985.
(29) Hendriks, K.; Heintges, G. H. L.; Wienk, M. M.; Janssen, R. A. J. Comparing Random and Regular Diketopyrrolopyrrole-Bithiophene-Thienopyrrolodione Terpolymers for Organic Photovoltaics. *J. Mater. Chem. A* **2014**, *2*, 17899−17905.
(30) Kang, T. E.; Kim, K.-H.; Kim, B. J. Design of Terpolymers as Electron Donors for Highly Efficient Polymer Solar Cells. *J. Mater. Chem. A* **2014**, *2*, 15252−15267.
(31) Burkhart, B.; Khlyabich, P. P.; Thompson, B. C. Influence of the Acceptor Composition on Physical Properties and Solar Cell Performance in Semi-Random Two-Acceptor Copolymers. *ACS Macro Lett.* **2012**, *1*, 660−666.
(32) Burkhart, B.; Khlyabich, P. P.; Thompson, B. C. Semi-Random Two-Acceptor Polymers: Elucidating Electronic Trends Through Multiple Acceptor Combinations. *Macromol. Rapid Commun.* **2013**, *214*, 681−690.
(33) Burkhart, B.; Khlyabich, P. P.; Cakir Canak, T.; LaJoie, T. W.; Thompson, B. C. Semi-Random" Multichromophoric rr-P3HT Analogues for Solar Photon Harvesting. *Macromolecules* **2011**, *44*, 1242−1246.
(34) Nielsen, C. B.; Ashraf, R. S.; Schroeder, B. C.; D'Angelo, P.; Watkins, S. E.; Song, K.; Anthopoulos, T. D.; McCulloch, I. Random Benzotrithiophene-Based Donor−Acceptor Copolymers for Efficient Organic Photovoltaic Devices. *Chem. Commun.* **2012**, *48*, 5832−5834.
(35) Jiang, J.-M.; Chen, H.-C.; Lin, H.-K.; Yu, C.-M.; Lan, S.-C.; Liu, C.-M.; Wei, K.-H. Conjugated Random Copolymers of Benzodithiophene−Benzooxadiazole−Diketopyrrolopyrrole with Full Visible Light Absorption for Bulk Heterojunction Solar Cells. *Polym. Chem.* **2013**, *4*, 5321−5328.
(36) Jung, J. W.; Liu, F.; Russell, T. P.; Jo, W. H. Semi-Crystalline Random Conjugated Copolymers with Panchromatic Absorption for Highly Efficient Polymer Solar Cells. *Energy Environ. Sci.* **2013**, *6*, 3301−3307.
(37) Kang, T. E.; Cho, H.-H.; Kim, H. jun; Lee, W.; Kang, H.; Kim, B. J. Importance of Optimal Composition in Random Terpolymer-Based Polymer Solar Cells. *Macromolecules* **2013**, *46*, 6806−6813.
(38) Zhang, M.; Wu, F.; Cao, Z.; Shen, T.; Chen, H.; Li, X.; Tan, S. Improved Photovoltaic Properties of Terpolymers Containing Diketopyrrolopyrrole and an Isoindigo Side Chain. *Polym. Chem.* **2014**, *5*, 4054−4060.
(39) Khlyabich, P. P.; Burkhart, B.; Thompson, B. C. Efficient Ternary Blend Bulk Heterojunction Solar Cells with Tunable Open-Circuit Voltage. *J. Am. Chem. Soc.* **2011**, *133*, 14534−14537.
(40) Khlyabich, P. P.; Burkhart, B.; Thompson, B. C. Compositional Dependence of the Open-Circuit Voltage in Ternary Blend Bulk Heterojunction Solar Cells Based on Two Donor Polymers. *J. Am. Chem. Soc.* **2012**, *134*, 9074−9077.
(41) Street, R. A.; Davies, D.; Khlyabich, P. P.; Burkhart, B.; Thompson, B. C. Origin of the Tunable Open-Circuit Voltage in Ternary Blend Bulk Heterojunction Organic Solar Cells. *J. Am. Chem. Soc.* **2013**, *135*, 986−989.
(42) Khlyabich, P. P.; Rudenko, A. E.; Street, R. A.; Thompson, B. C. Influence of Polymer Compatibility on the Open-Circuit Voltage in Ternary Blend Bulk Heterojunction Solar Cells. *ACS Appl. Mater. Interfaces* **2014**, *6*, 9913−9919.
(43) Lu, L.; Xu, T.; Chen, W.; Landry, E. S.; Yu, L. Ternary Blend Polymer Solar Cells with Enhanced Power Conversion Efficiency. *Nat. Photonics* **2014**, *8*, 716−722.
(44) Chen, Y.-C.; Hsu, C.-Y.; Lin, R. Y.-Y.; Ho, K.-C.; Lin, J. T. Materials for the Active Layer of Organic Photovoltaics: Ternary Solar Cell Approach. *ChemSusChem* **2013**, *6*, 20−35.
(45) Yang, L.; Yan, L.; You, W. Organic Solar Cells Beyond One Pair of Donor−Acceptor: Ternary Blends and More. *J. Phys. Chem. Lett.* **2013**, *4*, 1802−1810.
(46) Ameri, T.; Heumüller, T.; Min, J.; Li, N.; Matt, G.; Scherf, U.; Brabec, C. J. IR Sensitization of an Indene-C_{60} Bisadduct (ICBA) in Ternary Organic Solar Cells. *Energy Environ. Sci.* **2013**, *6*, 1796−1801.
(47) Ameri, T.; Min, J.; Li, N.; Machui, F.; Baran, D.; Forster, M.; Schottler, K. J.; Dolfen, D.; Scherf, U.; Brabec, C. J. Performance Enhancement of the P3HT/PCBM Solar Cells Through NIR Sensitization Using a Small-Bandgap Polymer. *Adv. Energy Mater.* **2012**, *2*, 1198−1202.
(48) Yang, L.; Zhou, H.; Price, S. C.; You, W. Parallel-like Bulk Heterojunction Polymer Solar Cells. *J. Am. Chem. Soc.* **2012**, *134*, 5432−5435.
(49) Khlyabich, P. P.; Burkhart, B.; Rudenko, A. E.; Thompson, B. C. Optimization and Simplification of Polymer−Fullerene Solar Cells

DOI: 10.1021/am5066267
ACS Appl. Mater. Interfaces 2015, 7, 2322−2330

Through Polymer and Active Layer Design. *Polymer* **2013**, *54*, 5267−5298.
(50) Ameri, T.; Khoram, P.; Min, J.; Brabec, C. J. Organic Ternary Solar Cells: A Review. *Adv. Mater.* **2013**, *25*, 4245−4266.
(51) Li, H.; Zhang, Z.-G.; Li, Y.; Wang, J. Tunable Open-Circuit Voltage in Ternary Organic Solar Cells. *Appl. Phys. Lett.* **2012**, *101*, 163302.
(52) Xu, H.; Ohkita, H.; Benten, H.; Ito, S. Open-Circuit Voltage of Ternary Blend Polymer Solar Cells. *Jpn. J. Appl. Phys.* **2014**, *53*, 01AB10.
(53) Kang, H.; Kim, K.-H.; Kang, T. E.; Cho, C.-H.; Park, S.; Yoon, S. C.; Kim, B. J. Effect of Fullerene Tris-Adducts on the Photovoltaic Performance of P3HT:Fullerene Ternary Blends. *ACS Appl. Mater. Interfaces* **2013**, *5*, 4401−4408.
(54) Deibel, C.; Strobel, T.; Dyakonov, V. Role of the Charge Transfer State in Organic Donor-Acceptor Solar Cells. *Adv. Mater.* **2010**, *22*, 4097−4111.
(55) Street, R. A.; Hawks, S.; Khlyabich, P. P.; Li, G.; Schwartz, B. J.; Thompson, B. C.; Yang, Y. The Electronic Structure and Transition Energies in Polymer-Fullerene Bulk Heterojunctions. *J. Phys. Chem. C* **2014**, *118*, 21873−21883.
(56) Ameri, T.; Khoram, P.; Heumüller, T.; Baran, D.; Machui, F.; Troeger, A.; Sgobba, V.; Guldi, D.; Halik, M.; Rathgeber, S.; Scherf, U.; Brabec, C. J. Morphology Analysis of Near IR Sensitized Polymer/Fullerene Organic Solar Cells by Implementing Low Bandgap Heteroanalogues C-/Si-PCPDTBT. *J. Mater. Chem. A* **2014**, *2*, 19461−19472.
(57) Khlyabich, P. P.; Burkhart, B.; Ng, C. F.; Thompson, B. C. Efficient Solar Cells from Semi-Random P3HT Analogues Incorporating Diketopyrrolopyrrole. *Macromolecules* **2011**, *44*, 5079−5084.
(58) Bulliard, X.; Ihn, S.-G.; Yun, S.; Kim, Y.; Choi, D.; Choi, J.-Y.; Kim, M.; Sim, M.; Park, J.-H.; Choi, W.; Cho, K. Enhanced Performance in Polymer Solar Cells by Surface Energy Control. *Adv. Funct. Mater.* **2010**, *20*, 4381−4387.
(59) Sun, Y.; Chien, S.-C.; Yip, H.-L.; Chen, K.-S.; Zhang, Y.; Davies, J. A.; Chen, F.-C.; Lin, B.; Jen, A. K.-Y. Improved Thin Film Morphology and Bulk-Heterojunction Solar Cell Performance Through Systematic Tuning of the Surface Energy of Conjugated Polymers. *J. Mater. Chem.* **2012**, *22*, 5587−5595.
(60) Kokil, A.; Yang, K.; Kumar, J. Techniques for Characterization of Charge Carrier Mobility in Organic Semiconductors. *J. Polym. Sci., Part B: Polym. Phys.* **2012**, *50*, 1130−1144.
(61) Li, A.; Amonoo, J.; Huang, B.; Goldberg, P. K.; McNeil, A. J.; Green, P. F. Enhancing Photovoltaic Performance Using an All-Conjugated Random Copolymer to Tailor Bulk and Interfacial Morphology of the P3HT:ICBA Active Layer. *Adv. Funct. Mater.* **2014**, *24*, 5594−5602.
(62) De Wit, J.; Van Ekenstein, G. A.; Polushkin, E.; Korhonen, J.; Ruokolainen, J.; Ten Brinke, G. Random Copolymer Effect in Self-Assembled Hydrogen-Bonded P(S-C-4VP)(PDP) Side-Chain Polymers. *Macromolecules* **2009**, *42*, 2009−2014.
(63) Huang, J.-H.; Hsiao, Y.-S.; Richard, E.; Chen, C.-C.; Chen, P.; Li, G.; Chu, C.-W.; Yang, Y. The Investigation of Donor-acceptor Compatibility in Bulk-heterojunction Polymer Systems. *Appl. Phys. Lett.* **2013**, *103*, 043304.
(64) Honda, S.; Ohkita, H.; Benten, H.; Ito, S. Selective Dye Loading at the Heterojunction in Polymer/Fullerene Solar Cells. *Adv. Energy Mater.* **2011**, *1*, 588−598.
(65) Xu, H.; Ohkita, H.; Hirata, T.; Benten, H.; Ito, S. Near-IR Dye Sensitization of Polymer Blend Solar Cells. *Polymer* **2014**, *55*, 2856−2860.
(66) Van Bavel, S.; Veenstra, S.; Loos, J. On the Importance of Morphology Control in Polymer Solar Cells. *Macromol. Rapid Commun.* **2010**, *31*, 1835−1845.
(67) Dang, M. T.; Hirsch, L.; Wantz, G.; Wuest, J. D. Controlling the Morphology and Performance of Bulk Heterojunctions in Solar Cells. Lessons Learned from the Benchmark Poly(3-hexylthiophene):[6,6]-Phenyl-C_{61}-Butyric Acid Methyl Ester System. *Chem. Rev.* **2013**, *113*, 3734−3765.
(68) Kotlarski, J. D.; Moet, D. J. D.; Blom, P. W. M. Role of Balanced Charge Carrier Transport in Low Band Gap Polymer:Fullerene Bulk Heterojunction Solar Cells. *J. Polym. Sci., Part B: Polym. Phys.* **2011**, *49*, 708−711.
(69) Savoie, B. M.; Dunaisky, S.; Marks, T. J.; Ratner, M. A. The Scope and Limitations of Ternary Blend Organic Photovoltaics. *Adv. Energy Mater.* **2014**, DOI: 10.1002/aenm.201400891.

DOI: 10.1021/am5066267
ACS Appl. Mater. Interfaces 2015, 7, 2322−2330